Journal of Neuroscience Methods 311 (2019) 351–359

Contents lists available at ScienceDirect

Journal of Neuroscience Methods

journal homepage: www.elsevier.com/locate/jneumeth

Electrophysiological signatures of the resting-state fMRI global signal: A simultaneous EEG-fMRI study

Xiaoli Huang[a,b], Zhiliang Long[a,b], Xu Lei[a,b,c,d,*]

[a] Sleep and NeuroImaging Center, Faculty of Psychology, Southwest University, Chongqing, 400715, China
[b] Key Laboratory of Cognition and Personality of Ministry of Education, Chongqing, 400715, China
[c] Key Laboratory for NeuroInformation of Ministry of Education, Center for Information in Medicine, University of Electronic Science and Technology of China, Chengdu, 610054, China
[d] Chongqing Collaborative Innovation Center for Brain Science, Chongqing, 400715, China

ARTICLE INFO

Keywords:
Global signal
Simultaneous EEG-fMRI
Reference electrode standardization technique

ABSTRACT

Background: The global signal of resting-state functional magnetic resonance imaging (fMRI) constitutes an intrinsic fluctuation and presents an opportunity to characterize and understand the activity of the whole brain. Recently, evidence that the global signal contains neurophysiologic information has been growing, but the global signal of electroencephalography (EEG) has never been determined.

New methods: We developed a new method to obtain the EEG global signal. The EEG global signal was reconstructed by the reference electrode standardization technique and represented the outer cortical electrophysiological activity. To investigate its relationship with the global signal of resting-state fMRI, a simultaneous EEG-fMRI signal was recorded, and this was analyzed in 24 subjects.

Results: We found that the global signal of resting-state fMRI showed a positive correlation with power fluctuations of the EEG global signal in the γ band (30–45 Hz) and a negative correlation in the low-frequency band (4–20 Hz).

Comparison with existing method(s): Compared with the global signal of fMRI, the global signal of EEG provides more temporal information about outer cortical neural activity.

Conclusions: These results provide new evidence for the electrophysiology information of the global signal of resting-state fMRI. More importantly, due to its high correlation with the fMRI global signal, the EEG global signal may serve as a new biomarker for neurological disorders.

1. Introduction

The fMRI global signal (GS) refers to the average time series of blood oxygen level dependent (BOLD) signal of all voxels in the whole brain (Zarahn et al., 1997). Previous research has suggested that GS is a nuisance regressor, mainly due to the disruption caused by its effects, including head motion, respiration, cardiac effects, and even interference from the MRI system (Bianciardi et al., 2009; Power et al., 2016; Yan et al., 2009). To improve the quality of the signal, the global signal has been considered a covariate, and it has been removed from the BOLD signal. An interesting consequence after global signal regression (GSR) is an increase in the degree of inverse correlation between the default mode network (DMN) and dorsal attention network (DAN) (Fox et al., 2005).

However, there is growing evidence that the GS is not noise but that it contains valuable information, and many neuroscientists argue strongly against the use of GSR (Murphy and Fox, 2016; Power et al., 2016; Saad et al., 2012; Yeo et al., 2015). First, many studies suggested that the GS is state dependent. For example, some behavioral interventions, such as sleep deprivation, can greatly change the amplitude of the GS, and GSR during preprocessing would interfere with the comparison between the sleep deprivation and normal sleep groups (Yeo et al., 2015). Second, a series of other studies based on simultaneous EEG-fMRI recording indicated that the GS fluctuation is negatively correlated with the EEG measures of vigilance (Wong et al., 2016, 2012; Wong et al., 2013). Third, the GS also differs between normal persons and patients with mental illness, and it may carry diagnostic information. Yang et al. (2014) compared schizophrenia patients to healthy subjects and people diagnosed with bipolar disorder by using biologically informed computational modeling and found that the variance of the GS was significantly higher in the schizophrenia patients. The increase in variance reflected the growth of the self-coupling of local

* Corresponding author at: Sleep and NeuroImaging Center, Faculty of Psychology, Southwest University, Chongqing, 400715, China.
E-mail address: xlei@swu.edu.cn (X. Lei).

https://doi.org/10.1016/j.jneumeth.2018.09.017
Received 19 June 2018; Received in revised form 10 September 2018; Accepted 14 September 2018
Available online 17 September 2018
0165-0270/

nodes and the global coupling between distant nodes. A further study found that the topography of the GS served as a robust clinical marker in schizophrenia and that it could be used as a diagnostic tool (Yang et al., 2016). Moreover, GSR has a certain impact on data analysis. For instance, it would incur aberrant correlation patterns and distorted intergroup differences (Fox et al., 2009; Murphy et al., 2009; Saad et al., 2012), and it would reduce the test-retest reliability of the salience network estimation in two scans with an interval of a year (Guo et al., 2012).

Recently, multimodal neuroimaging was employed to identify the neurophysiologic signature of the GS. Lachaux et al. (2007) found that fMRI activations were closely linked with EEG γ band activations spatially. They combined fMRI and intracranial EEG recordings of epileptic patients performing a semantic decision task. For a visual attention task, a simultaneous EEG-fMRI study further reported that trial-by-trial BOLD fluctuations were positively correlated with trial-by-trial fluctuations in the EEG γ band (Scheeringa et al., 2011). An animal study using combined LFP and fMRI indicated that the γ band of local field potential (LFP) power was positively correlated with fMRI signals over the cortex, indicating that the GS was tightly coupled with the underlying neural activity (Schölvinck et al., 2010). In summary, all of these studies point to the fact that the power of a particular frequency band, namely, the γ band, has a relatively high correlation with the GS (Lachaux et al., 2007; Schölvinck et al., 2010; Scheeringa et al., 2011). However, many other simultaneous EEG-fMRI studies indicated an opposite change in vascular and electrical activity (Lenkov et al., 2013; Middlebrooks et al., 2017; Mcsweeney et al., 2017), which suggests that there may different EEG-fMRI relationships that need to be considered when the cortex and subcortex structures are interpreted (Mishra et al., 2011).

What is the EEG global signal? An intuitive answer to this might be the average signal of all of the channels. However, an obstacle to this is that the EEG signal must be quantified as a potential difference from a reference channel. If the EEG global signal is obtained by calculating the average of all original online signals, it will depend strongly on the signal from the reference channel. For practical application, this average signal is always subtracted from each channel, i.e., the so-called “average reference” in the field of EEG study. The average reference as an easy-to-use method is widely adopted. Theoretically, the common average of all recorded EEG activity will approximately equal zero if the spatial sampling sufficiently covers a whole spherical head surface with sufficient density (Bertrand et al., 1985; Nunez and Srinivasan, 2006; Yao, 2017). Practically, EEG recordings are usually based on the hemi-head (the upper part of the head) electrode array. The average signal is definitively not zero, and we use this average signal as the practical global electrophysiology signal. However, it seems impossible to obtain an absolute measure of the global electrophysiology signal from scalp EEG because there is no way to find a neutral or “quiet” reference location. When the average reference is adopted, this global signal gets lost during subtraction. Fortunately, the reference electrode standardization technique (REST) proposed by Yao can transform the EEG signal into the potentials referenced to a point located at infinity (Yao, 2001), and it provides a way to obtain the global electrophysiology signal from scalp EEG. When reconstructing the equivalent source, the potentials referenced at infinity are approximately calculated from the equivalent sources. In the present study, we developed a signal, the average signal after re-reference of REST (see Methods for more detail), as the infinite-reference yielded average oscillation (YAO) signal. The YAO signal is the average electrical activity reconstructed from the scalp EEG, regardless of which original reference it used. Considering its similarity to the GS of fMRI, we considered the YAO signal as the EEG global signal. It is worth noting that the YAO signal reflects only the electrical signals of the outer cortex. It may not include the electrical activity in the subcortical structure.

In a study of simultaneous intracortical recordings of neural signals and fMRI responses, the high-frequency band of LFP power, namely, the γ rhythm, could predict the activation of the BOLD signal (Logothetis et al., 2001), and this association was extended to the GS of fMRI, as the resting-state data indicated its positive correlation with the LFP-measured spontaneous fluctuations in a single cortical site (Schölvinck et al., 2010). Here, because the YAO signal is the average electrical activity of the whole-brain with a reference at a point of infinity, we speculated that the YAO signal was equivalent to the fMRI GS and that the power of high frequency band, i.e., the γ band, had a positive correlation with the GS. In the present study, a simultaneous EEG-fMRI recording was performed to collect the resting-state data from 24 subjects and to explore the relationship between the YAO signal of EEG and the global signal of fMRI. Specifically, we hoped to address the following questions: What are the spectrum properties of the YAO signal? Is there any linear correlation between the YAO signal and the global signal of fMRI, especially in the γ band? If so, what is the relation in other frequency bands of the YAO signal?

2. Methods

2.1. Subjects

Twenty-four college students, ranging from 18 to 25 years in age (mean ± std: 21.4 ± 2 years; 12 males) were recruited through online advertisement. All subjects had normal or corrected-to-normal vision and had no history of psychiatric or neurological illness when evaluated by the psychiatric clinical assessment. This study was approved by the ethics committee of Southwest University, and consent to participate in the study was received from the subjects. The 24 students received a monetary reward after they completed the study. The study contained an eyes-open (EO) and an eyes-closed (EC) five-minute resting state. Under the EO condition, the subjects were requested to concentrate on the "+" in the middle of the screen, while in the EC condition, they were informed that they needed to calm their mind into a relaxed state and avoid consciously thinking about something.

2.2. Acquisition of MRI data

The whole-brain resting-state BOLD signals were acquired by a 3 T Siemens Trio scanner. There were 200 functional volumes obtained in each period with a T2-weighted gradient-echo planar imaging (EPI) sequence (TR/TE = 1500/29 ms, FOV = 192 × 192 mm^2, flip angle = 90°, acquisition matrix = 64 × 64, thickness/gap = 5/0.5 mm, in-plane resolution = 3.0 × 3.0 mm^2, axial slices = 25). Finally, there was an acquisition of T1 that continued for 5 min, and no other instructions were given except to keep relaxed and hold still. With the 3D spoiled gradient-echo (SPGR) sequence (TR/TE = 8.5/3.4 ms, FOV = 240 × 240 mm^2, flip angle = 12°, acquisition matrix = 512 × 512, thickness/gap = 1/0 mm), the whole-brain structural image was acquired. The high-resolution T1-weighted structural volume provided an anatomical reference for the functional scan. Head movements were minimized by using a cushioned head fixation device.

2.3. Acquisition of EEG data

The Brain Products system was used for EEG data collection in the present study (BrainAmp MR plus, Brain Products, Munich, Germany). Thirty-two Ag/AgCl channels were placed on the scalp, and the channel position was in accordance with the International 10–20 System. All impedances were below 10 kΩ. The amplifier was a nonmagnetic MRI-compatible EEG system. The FCz point was used as the reference for online signal collection, and the sampling rate was 5 kHz. The EEG amplifier was charged by a rechargeable power pack placed outside the scanner bore. To ensure the temporal stability of the EEG acquisition in relation to the switching of the gradients during the MR acquisition, we used a SyncBox (SyncBox MainUnit, Brain Products GmbH, Gilching,

Germany) to synchronize the amplifier system with the MRI scanner's system. The amplified and digitized EEG signal was transmitted to the recording computer with fiber optic cables. The computer was placed outside the scanner room and the Adapter (BrainAmp USB-Adapter, Brain products, Gilching, Germany) converted optical signal into electrophysiology signal.

2.4. fMRI preprocessing

The fMRI data were preprocessed using SPM8 (http://www.fil.ion.ucl.ac.uk/spm/), which was developed by the Welcome Department of Cognitive Neurology, London, UK. The preprocessing steps included slice timing, head motion correction, spatial normalization, and smoothing (6 mm full-width at half-maximum Gaussian kernel). None of the subject's head motions exceeded 3 mm. Based on the whole-brain template (threshold: 0.1) from SPM, global signal (GS) was extracted. At the same time, we used the gray matter template (threshold: 0.6) from SPM to obtain an alternative version of the GS: the global signal of the gray matter. Considering the contribution of white matter and cerebrospinal fluid (CSF), these covariates were obtained by using the white matter and CSF template of SPM. In the subsequent analysis, these covariates, additionally including 6 head motion parameters, were regressed as interference factors.

2.5. Estimation of the YAO signal

As illustrated in Fig. 1, the EEG preprocessing contained a series of crucial steps to obtain the predictor of each band for the fMRI global signal. Each step was described in detail as follows (see Fig. 1).

Step 1: MRI artifact correction. According to the average template subtraction procedure, we first removed the fMRI gradient and ballistocardiographic artifacts from the original EEG signal (Allen et al., 2000; Niazy et al., 2005). Then, the EEG data were downsampled to 250 Hz and digitally filtered within the 0.1–45 Hz frequency band using a Chebyshev II-type filter. The residual fMRI gradient and ballistocardiographic artifacts, ocular artifacts and the muscle activity artifact from the EEG data were further eliminated through temporal independent component analysis (ICA). The filtered EEG recordings were re-referenced to the average reference for further analyses. All of these processes were implemented with Vision Analyzer software (Version 2.0, Brain Products, Inc., Munich, Germany), and more details on this were given in Supplementary Materials.

Step 2: estimation of the YAO signal. The average-referenced EEG signals were further processed with reference electrode standardization technique (REST) software (http://www.neuro.uestc.edu.cn/rest) (Dong et al., 2017). REST translated the artifact-corrected signal into another signal with the reference of a point at infinity by a transfer matrix (Yao, 2001). The head model and equivalent source model were the key components in estimating the transfer matrix, and we chose the three-concentric-sphere model and equivalent source model provided in the software (Dong et al., 2017). Then, the reconstructed signals of all channels were averaged to obtain a new signal of a virtual channel, namely, the infinite-reference yielded average oscillation (YAO) signal. Basically, the YAO signal is the vector V' as per the original paper by (Yao, 2001). The YAO signal represents the outer cortical electrophysiological activity. To estimate the YAO signal, here, we recommend using a number of channels more than 32 and using channels that cover the upper part of the head.

Step 3: calculation of the band power. The YAO signal was epoched to 1.5 s, corresponding to the TR of our fMRI acquisition. Using fast Fourier transform, we calculated the power in seven frequency bands: δ (2–4 Hz), θ (4–8 Hz), α1 (8–10.5 Hz), α2 (10.5–13 Hz), β1 (13–20 Hz), β2 (20–30 Hz), and γ (30–45 Hz). To approximate a normal distribution, the power value was transformed into logarithms ($10 \times \log_{10}(\mu v^2/Hz)$) before statistical analysis was performed. Because of the remnants of the gradient artifact, micromovements and muscle activity, epochs of power appearing to contain artifacts by visual inspection, were discarded and replaced by interpolating the band power linearly between segments before and after the artifacts.

Step 4: convolution of the hemodynamic response function with band power. The band power curves of the YAO signal were convolved with the canonical hemodynamic response function (HRF). This HRF comprised the sum of two gamma functions and was the default option in SPM (Friston et al., 1998). The canonical HRF exhibited a rise peaking approximately 5 s, followed by an undershoot. Then, the HRF-convolved band power curves were correlated with the fMRI global signal. We calculated the correlation coefficient for each band in each subject, and these coefficients were further transformed by Fisher's r-to-z to improve their normality. We conducted a one-sample *t*-test to check whether there was consistent correlation between the EEG band power and the fMRI global signal. As all of the above analyses were exploratory studies, all of the p-values were uncorrected for multiple tests. However, we also reported the Bonferroni-corrected results of our major results.

2.6. Statistical comparisons

The YAO signal, which was generated after the re-reference of REST was performed, was a new signal representing the average global electrical activity. To explore the relationship between the YAO signal and the signal of each channel, we used fast Fourier transform to calculate the power of the YAO signal across frequencies on each subject. Meanwhile, the power of each channel in each frequency band was calculated, and the mean power of all the channels were calculated to obtain the grand average power (GAP). In Supplementary Fig. S1, the data flow diagram for calculating the grand average power and the power of the YAO signal is illustrated. It should be noticed that the two power were constructed based on the average-referenced signal, and both describe the neural activity band power of the outer cortex. 2 (signal types: YAO or GAP) × 7 (frequency bands) ANOVA was applied separately in the EO and EC conditions (see Fig. 2A, B).

2.7. Complementary analyses

To test the replicability of the research, we conducted several complementary analyses. For the fMRI global signal, we extracted the signal of the whole brain and, at the same time, considered the signal from the gray matter, which greatly reduced the effect of white matter. We further employed the subject's individual segmentation of gray matter to increase the accuracy of the global signal estimation. We used the modified Gaussian mixture model in SPM to segment MR images into different tissue classes. This algorithm can produce a more robust classification based on the prior spatial probability of each voxel from gray matter, white matter or cerebrospinal fluid (Ashburner and Friston, 2005). For the EEG global signal, an alternative choice was the band power of each channel after the average-reference was computed. In this analysis, the signal of each channel was epoched to 1.5 s, and then, the band power was calculated in each epoch and logarithmically transformed. Because of the low signal-to-noise ratio for a single channel, we automatically discarded the time point with an artifact and replaced it by an interpolating one (the same procedure described in Step 3). The artifact time point was defined as the absolute amplitude 2.5 times larger than the median amplitude. The number of the artifact time points on a channel for each participant ranged from 1 to 23 (mean ± std = 11.2 ± 5.2). Each channel corresponded with a time course in each frequency band, and the correlation coefficient of it with the fMRI global signal was calculated for each band in each channel. This analysis would indicate the spatial distribution of the fMRI global signal in the scalp surface.

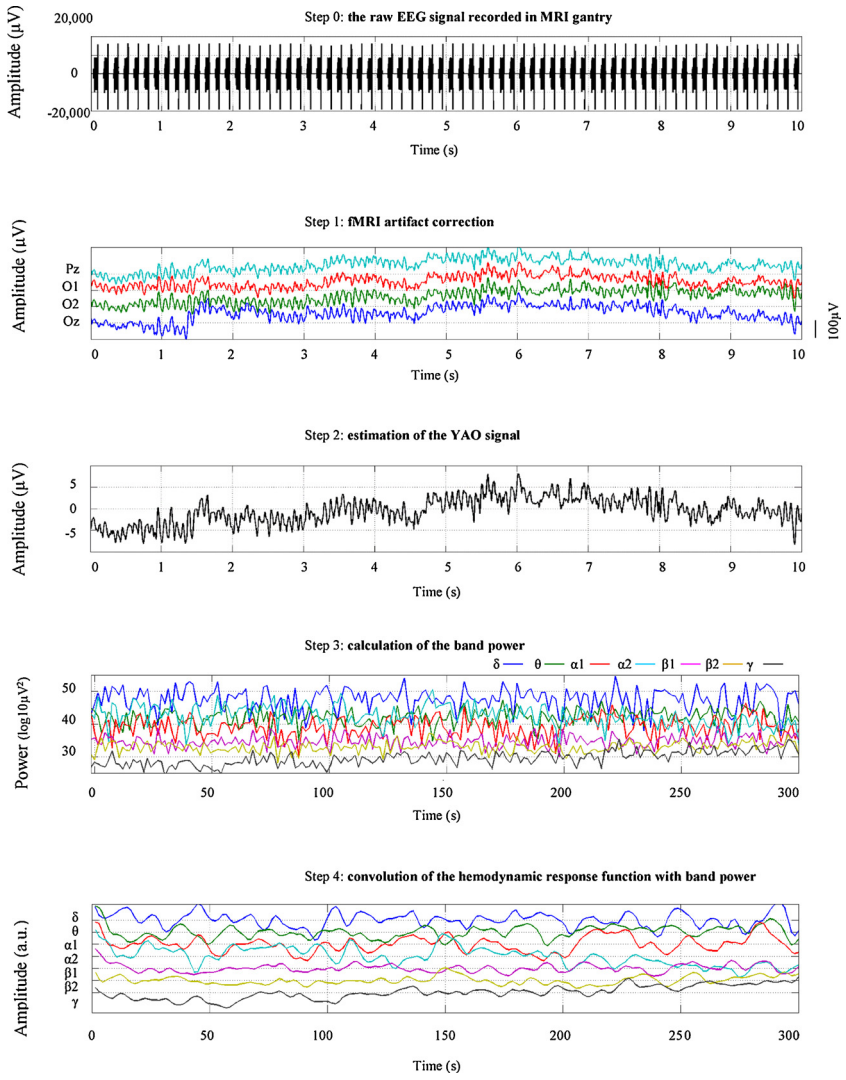

Fig. 1. The flow diagram of data analysis. Step 0: the raw EEG signal recorded in MRI gantry; Step1: EEG cleaned of the fMRI gradient and ballistocardiographic artifacts; Step 2: the amplitude profile of the YAO signal oscillations in a time window of 10 s; Step 3: the band power of all the seven rhythms over the entire session in the time window of 300 s; Step 4: the time courses of seven band power after convolution with the hemodynamic response function.

3. Results

3.1. Spectrum properties of the YAO signal

In the EO condition, the main effects of the signal types and frequency bands were significant ($F(2.28, 52.48) = 171.77$, $p < 0.001$; $F(1, 23) = 187.13$, $p < 0.001$), and the interaction within the two factors was significant too ($F(3.16, 72.77) = 9.68$, $p < 0.001$). In the EC condition, we had similar results: the main effects for signal types ($F(1, 23) = 288.49$, $p < 0.001$), frequency bands ($F(2.65, 60.91) = 216.27$, $p < 0.001$), and interaction ($F(3.31, 76.09) = 18.16$, $p < 0.001$) were significant. These results illustrated that the YAO signal was not simply the linear weighting of the grand average power of all of the scalp channels but that it differed in frequencies of both EO and EC conditions. We calculated the correlation coefficients between the two signals in each frequency band, and they were highly related to the total (see Fig. 2C, D). The range of the correlation coefficient was 0.4353–0.7896, corresponding to β1 ($p = 0.0335$) in the EC condition and to γ ($p < 0.001$) in the bands in the EO condition (Fig. 2). As α rhythm is the dominate rhythm for the comparison between the EO and EC conditions, we conducted separate t-tests between these conditions in the YAO signal and found the reserved larger value of α1 rhythm in the EC condition ($t = 2.016$, $p = 0.028$), but it was not significant for α2 ($t = 1.396$, $p = 0.088$, see Supplementary Fig. S2).

3.2. Correlation between HRF-convolved YAO signal and fMRI global signal

Correlation analyses were applied between the HRF-convolved band power of the YAO signal and that of the fMRI global signal, as illustrated in Fig. 3 and Table 1. In the EC condition, there was a significant positive correlation between the γ band of the YAO signal and the fMRI global signal ($r = 0.667$, $p < 0.001$, Supplementary Fig. S3). In the other frequency bands, ranging from θ to β1, inverse correlation existed (θ, $r = -0.450$, $p < 0.001$; α1, $r = -0.296$, $p = 0.003$; α2, $r = -0.326$, $p < 0.001$; β1, $r = -0.201$, $p = 0.003$). However, there was no significant correlation in the frequency bands of δ ($r = -0.183$, $p = 0.033$) or β2 ($r = 0.086$, $p = 0.211$). There were similar strong correlations in the EO condition, especially in γ ($r = 0.232$, $p = 0.003$). In short, our data demonstrated that the YAO signal had opposite relationships to the fMRI global signal in two broad frequency domains: (i) a low-frequency band (4–20 Hz) with slightly negative correlation, and (ii) a high-frequency band (γ, 30–45 Hz) that showed a consistent positive correlation in both the EO and EC conditions (Fig. 3 and Table 1).

Because gray matter is the main contributor to the BOLD signal, we alternatively used the template of gray matter to extract the global

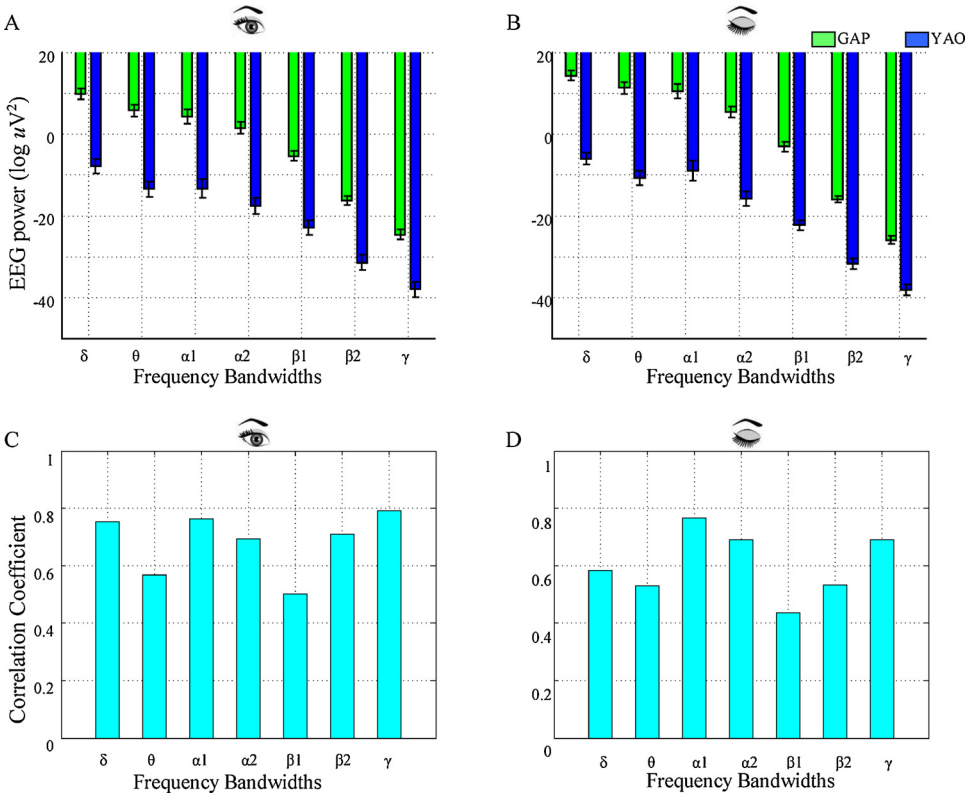

Fig. 2. The comparison of the power of YAO signal and the grand average power (GAP) of all the channels. (A) In the EO condition, (B) in the EC condition, the grand average power (green) and the power of YAO signal (blue). ANOVA tests found Yao signal had lower power, and their interaction with frequency bands was significant. (C) In the EO condition, (D) in the EC condition, the grand average power was highly related with the power of YAO signal in all frequency bands. The bars and the error bar stand for mean and standard error. (For interpretation of the references to colour in this figure legend, the reader is referred to the web version of this article.)

signal. The result was similar to that based on the template of the whole brain even further employed the subject's individual segmentation of gray matter (see Supplementary Table S1 for more information). We also considered the contribution of different subbands of the fMRI global signal in the correlation to the EEG signal, as all frequency bands below 0.33 Hz (TR = 1.5 s) may contribute to the strong correlation observed. The result was very similar to the band of 0-0.01 Hz (Supplementary Table S1). However, in a condition of the band of 0.01–0.08 Hz, which was considered the main contribution to the fMRI signal, the correlation disappeared, and the mean correlation ranged from −0.1847 to 0.1685 among different EEG frequency bands. We further analyzed the correlation between the power of each channel and the fMRI global signal. The result indicated that the correlation with each single channel was also significant. As illustrated in Fig. 4, in the EC and EO conditions, the range of the correlation with each channel after the average reference was from −0.3514 (θ band) to 0.6265 (γ band) (Fig. 4).

4. Discussion

We aimed to investigate how changes in the average electrophysiology activity of the whole scalp in different frequency bands were related to the global signal of resting-state fMRI. Here, we developed a new signal to represent the global electrophysiology signal referenced to a point at infinity, i.e., the YAO signal. One important finding of this study is that the HRF-convolved γ band (30–40 Hz) of the YAO signal was positively correlated with the global signal of fMRI (0-0.33 Hz), both in the eyes-closed (EC) and eyes-open (EO) conditions. Inversely, the low frequency band (4–20 Hz) of the YAO signal was negatively correlated with the global signal. Our findings implied that the YAO

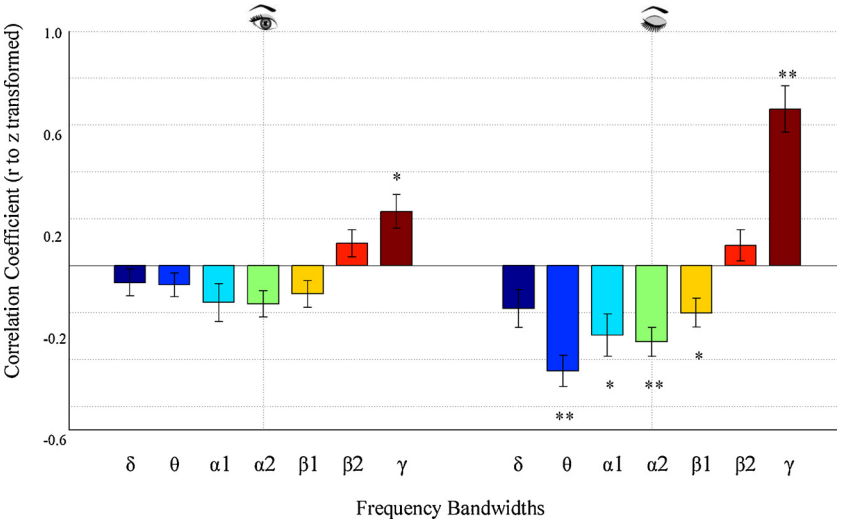

Fig. 3. Correlation between the YAO signal of scalp EEG and fMRI global signal. The left panel is for the EO condition, and the right is for the EC condition. In the EO condition, the α2 band was correlated negatively with the fMRI global signal ($r = -0.163$, $p = 0.008$) while the γ band positively ($r = 0.232$, $p = 0.003$). In the EC conditions, the low frequency bands (θ, α1, α2, and β1) showed negative correlation with GS ($r = -0.4450$, $p < 0.001$; $r = -0.296$, $p = 0.003$; $r = -0.325$, $p < 0.001$; $r = -0.201$, $p = 0.003$ respectively) while the γ band had significant positive correlation ($r = 0.667$, $p < 0.001$). The bars and the error bar stand for mean and standard error. * represent $p < 0.05$ and ** represent $p < 0.01$ after Bonferroni correction.

Table 1
Correlation between the HRF-convolved band power of YAO signal of EEG and fMRI global signal in eyes-closed and eyes-open conditions. The results for each frequency band (δ, θ, α1, α2, β1, β2, γ) and each subject were listed. The descriptive statistic (mean, stand deviation, *t*- and p-value) were listed in the last four rows. Boldfaced values represented the significant correlation after Bonferroni correction ($p < 0.05/14$). The original correlation coefficient was Fisher's r-to-z transformed to improve their normality.

subject	Eyes-open							Eyes-closed						
	δ	θ	α1	α2	β1	β2	γ	δ	θ	α1	α2	β1	β2	γ
1#	−0.428	−0.312	−0.308	−0.211	0.309	0.266	0.134	−0.440	−0.297	−0.492	−0.457	−0.147	0.232	0.685
2#	−0.668	−0.468	−0.521	−0.411	−0.297	0.503	0.650	0.142	−0.588	−0.418	−0.040	0.107	−0.028	0.611
3#	−0.172	−0.472	0.347	−0.165	−0.560	0.345	0.341	−0.652	−0.546	0.204	−0.279	0.071	−0.011	0.808
4#	−0.148	−0.269	−0.217	0.009	0.172	0.164	0.133	−0.334	−0.095	−0.331	−0.472	−0.542	0.291	0.633
5#	0.215	−0.098	−1.227	−0.544	−0.251	0.742	0.700	−0.864	−0.438	−0.236	−0.389	−0.348	0.110	1.014
6#	−0.414	−0.281	−0.167	0.020	−0.107	−0.104	0.558	−0.790	−0.842	−0.526	−0.263	−0.344	0.560	0.984
7#	0.003	0.130	0.204	−0.525	−0.154	0.066	0.098	0.211	−0.206	−0.646	−0.024	−0.043	−0.135	0.419
8#	0.586	0.212	0.429	0.322	−0.458	−0.439	−0.199	0.593	0.410	0.588	−0.308	0.016	−0.559	−0.299
9#	0.000	−0.045	−0.190	0.188	0.056	0.366	−0.341	0.192	−0.447	−1.028	−0.641	−0.914	0.147	1.313
10#	0.049	−0.074	0.241	0.349	−0.232	0.017	−0.120	−0.257	−0.369	−0.097	0.031	−0.022	0.215	0.153
11#	−0.414	−0.305	−0.139	−0.167	−0.429	0.092	0.741	−0.353	−0.653	−0.210	−0.189	0.012	−0.145	0.489
12#	−0.300	0.232	−0.249	−0.123	0.340	−0.392	0.271	0.479	−0.243	−0.593	−0.397	−0.134	0.310	0.310
13#	0.309	0.379	0.419	0.111	−0.068	−0.119	−0.492	−0.282	−0.522	−0.621	−0.424	0.379	0.292	0.685
14#	−0.218	−0.146	−0.179	−0.145	−0.061	−0.103	0.314	−0.511	−0.742	−0.489	−0.362	−0.138	0.075	1.175
15#	0.195	0.031	0.002	−0.361	−0.558	0.090	0.259	−0.197	−0.156	0.408	0.258	−0.637	−0.002	0.340
16#	0.067	−0.059	−0.357	−0.723	−0.291	0.507	0.337	−0.038	0.029	0.537	0.231	−0.066	−0.128	−0.253
17#	−0.129	0.030	0.174	0.041	0.171	−0.122	−0.071	−0.091	−0.492	−0.363	−0.183	−0.276	−0.223	1.057
18#	0.058	0.049	−0.222	−0.143	0.507	0.044	−0.280	−0.715	−1.031	−0.567	−0.707	−0.759	0.690	1.571
19#	−0.119	0.121	−0.049	−0.087	−0.284	−0.099	0.480	0.153	−0.530	−0.552	−0.839	−0.273	−0.811	1.196
20#	0.258	−0.189	−0.805	−0.466	0.105	0.188	0.402	0.455	−0.307	0.229	−0.706	0.147	0.261	0.043
21#	−0.233	−0.185	0.183	−0.053	−0.209	0.196	0.189	−0.321	−0.831	−1.063	−0.602	−0.165	0.368	0.996
22#	−0.204	−0.580	−0.672	−0.115	−0.097	0.206	0.720	−0.292	−0.859	0.021	−0.379	−0.123	0.209	0.700
23#	0.064	0.102	−0.413	−0.167	−0.251	−0.344	0.565	−0.296	−0.776	−0.171	−0.727	−0.461	−0.022	1.067
24#	−0.091	0.236	−0.063	−0.545	−0.243	0.208	0.172	−0.182	−0.264	−0.686	0.058	−0.165	0.374	0.320
mean	−0.072	−0.082	−0.157	−0.163	−0.120	0.095	0.232	−0.183	−0.450	−0.296	−0.325	−0.201	0.086	0.667
Std	0.278	0.248	0.396	0.276	0.280	0.288	0.348	0.396	0.326	0.444	0.302	0.299	0.328	0.481
t-value	−1.274	−1.613	−1.950	−2.891	−2.108	1.617	3.260	−2.262	−6.755	−3.262	−5.282	−3.290	1.287	6.798
p-value	0.215	0.120	0.063	0.008	0.046	0.120	**0.003**	0.033	< **0.001**	**0.003**	< **0.001**	**0.003**	0.211	< **0.001**

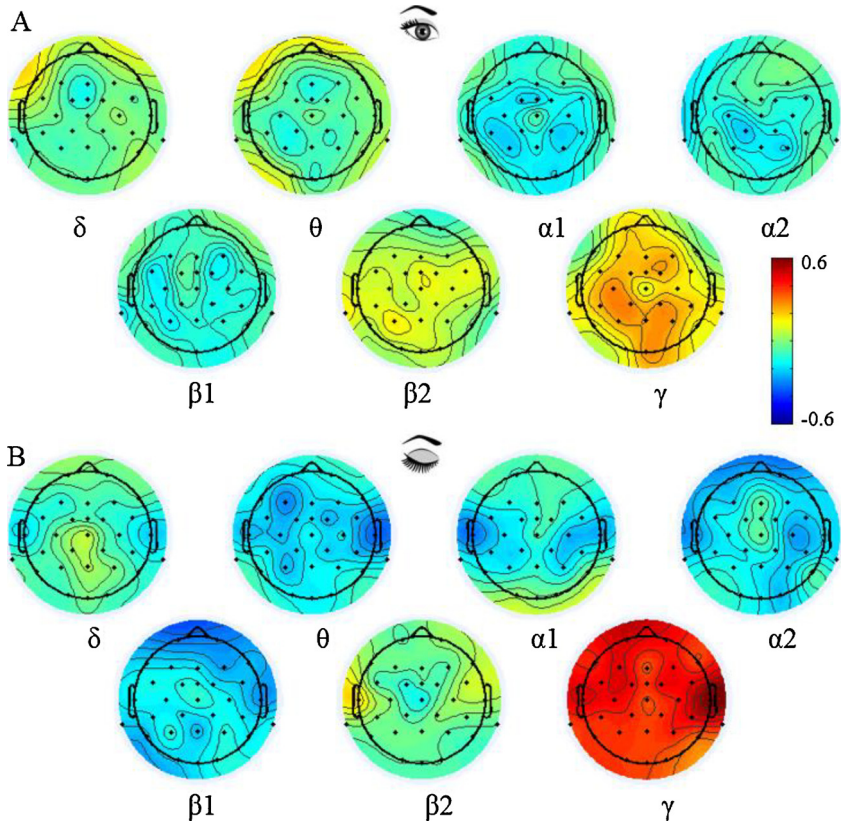

Fig. 4. Correlation between the fMRI global signal and single channel EEG with average reference. A. In the EO condition; B. in the EC condition. For both conditions, γ range showed a widespread correlation with fMRI global signal in the whole scalp surface.

signal might be the electrophysiology equivalence of the fMRI global signal. More importantly, our results provided new evidence for the neurophysiologic information of the global signal of fMRI.

4.1. The definition of the YAO signal

We tried to find an indicator to represent the global neural electrical activity. In practice, the widely accepted EEG references include earlobes, Cz and average reference methods, and they have certain adverse effects on scalp EEG recording (Goldman et al., 2002) because neural activity is a spatiotemporal process, and the electrical activity of the reference may influence the time domain of the EEG signal. To solve this problem, people try to find a point at which the reference potential is zero. However, it does not exist (Geselowitz, 1998). The reference electrode standardization technique (REST) can transform the original potential into a potential at infinity, regardless of which reference the original potential was based on. The physical basis is that the preceding and subsequent potentials of conversion are generated by the same source of actual nerve activity in the brain or their equivalent sources. More importantly, the estimated signal based on REST is not affected by the activity of the reference and the number of channels.

One of the main contributions of the present study is that it defined a new signal to represent the global signal of EEG, i.e., the YAO signal. This signal is based on the principle that the activity intensity of an equivalent source, which finally generates the recorded scalp EEG, is relative to infinity. By reconstructing the equivalent source, the potentials on the scalp are calculated approximately with a reference at infinity. Then, the signals of all the channels are averaged to obtain the YAO signal. Here, we practically defined the YAO signal as the direct current component of the spatial frequency spectrum of the upper part of the head. Theoretically, this signal definitely cannot be zero (Yao, 2017). Any regularly distributed montage, covering the upper part of the head, is acceptable for the estimation of the YAO signal. The International 10–20 system, which has a good coverage for the upper part of the head, is recommended for calculating the YAO signal. The high-density montage and realistic head model are both good choices because of their influences on the estimation of a neutral reference for EEG recordings (Liu et al., 2015).

An interesting contrast is the average reference. In the average reference, signals from all the channels are averaged and removed, i.e., the YAO signal is removed as an unwanted signal for the average reference. A very similar and dramatic scenario happened in the field of fMRI research: the fMRI global signal is regressed in fMRI data preprocessing, which is called GSR. Recently, growing research has realized that there is much neurophysiological information in the fMRI global signal. We thought the proposed YAO signal might be an efficient tool to identify useful information from the EEG signal. Since the fMRI global signal has been used as a diagnostic tool (Yang et al., 2016) and it has a close connection with the YAO signal, an optimistic expectation is that the YAO signal may be possible to play the same important role in diagnosis and treatment.

4.2. Spectrum properties of the YAO signal

Comparing the YAO signal between the EO and EC conditions, the YAO signal has a lower power than the grand average power of all channels. This would happen when the infinite referenced signal of a single channel was cancelled out during the calculation of the average. In EEG source space, the dipoles are distributed on gray matter, which can be approximated to one hemisphere (Brazier, 1966). Some dipoles point in the opposite directions when the reference is at infinity, so they may effectively cancel each other out. However, due to the existence of a significant interaction effect between frequency bands and signal types, the magnitude of decrease in the YAO signal varies for different frequency bands (see Fig. 2A and B). Hence, we speculated that the YAO signal was not a linear-filtered copy of the grand average power fluctuation of all channels. In addition, although all of the correlation values were greater than 0.4 (see Fig. 2C and D), with different rhythms, the correlation coefficients between the YAO signal and the grand average power of all channels were distinct, which indicated largely overlapped dynamic properties between the YAO signal and the signals from each channel.

4.3. The neurophysiological mechanism of the YAO signal and fMRI global signal

The main component of EEG is the total number of postsynaptic potentials in the cortex, which reflects the electrical changes of the scalp over a period of time (Nunez and Srinivasan, 2006). The LFP is the sum of postsynaptic potentials in the vicinity of the recording point, which reflects the local electrical changes of the neural network during a certain time (Kajikawa and Schroeder Charles, 2011; Mitzdorf, 1985). To some extent, both the LFP and EEG are direct measures of electrophysiological activity in different spatial scales of the brain. An absolute measure of the global electrophysiological signal from the scalp seems to be impossible to achieve today because of the inexistence of a neutral reference location. The reference electrode standardization technique (REST) provides a pathway to obtain the electrophysiological global signal from scalp EEG (Yao, 2001). By reconstructing the equivalent source, the potentials referenced at infinity are approximated from equivalent sources. The efficiency of REST has been repeatedly confirmed in several methodological studies (Lei and Liao, 2017; Liu et al., 2015). The YAO signal is independent from the reference, and it is the average electrical activity reconstructed from the scalp EEG, regardless of which original reference was used. Beyond that, the YAO signal represents the average of the outer cortex electrophysiological activity, and the underlying neurophysiological mechanism may be the same for the local LFP, though the former emphasizes a more macro level.

In contrast, the appearance of the BOLD signal relates to the blood oxygen surplus caused by the supply and consumption of blood oxygen. When nerve cells are active, their energy demand increases, which triggers a change in blood dynamics (Fox and Raichle, 1986; Fox et al., 1988). However, the BOLD signal is an indirect measurement of neural activities (Ogawa and Lee, 1990). Hence, the global signal, the average time series of the hemodynamic response should be an indirect measurement of neural activities of the whole brain. In addition, Logothetis et al. (2001) found that the BOLD signal was most closely related to the LFP. Considering the relationship between the LFP and EEG, it is reasonable to believe that the YAO signal has a certain corresponding relationship with the fMRI global signal and can be explained as an electrical equivalent of the global signal from the scalp. More importantly, both the YAO signal and fMRI global signal are generated mainly from gray matter, though the YAO signal is a concentrated expression of the outer cortical electrophysiological activity.

4.4. Electrophysiological signatures of the global signal

Another important finding of this study is that the HRF-convolved γ band (30–40 Hz) of the YAO signal was positively correlated with the fMRI global signal in both the EC and EO conditions. These results were supported by evidence from different spatial scales, including scalp EEG, the LFP and electrocorticography (ECoG). Mulert et al. (2010) used single-trial coupling of EEG and fMRI to investigate the relationship between BOLD and γ (40 Hz) amplitude during an auditory task and found positive correlations among the auditory cortex, thalamus and anterior cingulate cortex. After a year, Khursheed et al. (2011) found the amplitude of the ECoG γ band response was significantly positively correlated with the fMRI response during the delay periods of a working memory task. These findings were also consistent with previous reports of LFP coupling in the γ band with the fMRI signal (Logothetis et al., 2001). Another study that focused on the neural basis of global signal found that the high frequency part of the LFP

(40–80 Hz) had significant positive correlation with the fMRI signal over the whole cortex (Schölvinck et al., 2010). These findings demonstrated that the fMRI global signal fluctuation was tightly coupled with electrophysiological activity in the cerebral cortex.

In contrast to the positive correlation with the γ band, there were negative correlations between the global signal and the low-frequency bands of the YAO signal. Some previous simultaneous EEG-fMRI studies were dedicated to the spatial localization of α rhythm. They found the power fluctuation of α was negatively correlated with the BOLD signal in the whole neocortex and that it was positively correlated with deep brain regions, such as the thalamus and globus pallidus (Liu et al., 2012; Moosmann et al., 2003; Tyvaert et al. 2008). This inverse correlation was especially consistent in the visual cortex (Goldman et al., 2002). Due to the proportion of the deep brain region relative to the neocortex, the global signal is naturally more affected by the neocortex. Therefore, in this study, a negative correlation in α rhythm was observed in both the EO ($r = -0.163$, $p = 0.008$) and EC ($r = -0.325$, $p < 0.001$) conditions. In vigilance assessment, α rhythm plays an important role (Brookhuis and Waard, 1993). EEG vigilance was defined as the power of the α band divided by the power of the δ and θ bands (Horovitz et al., 2008; Olbrich et al., 2009). Some recent work has begun to focus on the amplitude of the global signal and EEG vigilance. In a simultaneous EEG-fMRI study of human subjects, Wong et al. (2013) found that the amplitude of the global signal was inversely correlated with EEG measures of vigilance. In addition, they found that increases in EEG vigilance measures associated with the ingestion of caffeine were significantly correlated with decreases in the fMRI global signal amplitude. In another study, Wong et al. (2016) further found that changes between the EO and EC resting-state conditions in the fMRI global signal amplitude were negatively correlated with the associated changes in EEG vigilance. Interestingly, the slope of the EO-EC relationship closely resembled that of the previously reported relationship between caffeine-related changes in the fMRI global signal amplitude and EEG vigilance. In these studies, there was a negative correlation between the fMRI global signal and EEG vigilance, that is, the larger the fMRI global signal was, the smaller the alertness and the power of α band was. Since no significant correlation was identified between the fMRI global signal and the δ or θ band in our current study, we rejected the alternative possibility of increased power of the δ or θ band related to a small vigilance.

In our study, the relationship between the fMRI global signal and the YAO signal was partially affected by the behavioral state, i.e., the EO and EC conditions. One possible reason for this is that as there were more blinks in the EO condition, the signal-to-noise ratio was smaller than that in the EC condition, and the preprocessing of artifact rejection was unable to remove its effect thoroughly. An alternative interpretation is that the coupling between the EEG and fMRI signals was influenced by alertness. In a previous study, because the signal of LFP was weakly affected by the artifacts of blinking, coupling between the LFP and fMRI signals over nearly the entire cerebral cortex was dependent on the monkey's behavioral state (Schölvinck et al., 2010). An obvious phenomenon was increased coupling between the LFP and fMRI signals when the animals' eyes were closed (Schölvinck et al., 2010). The behavior of the eyes implied a reaction and change of the arousal state in regards to the neurophysiological level (Abe et al., 2011). The mechanism of this phenomenon still needs to be explored further. It is worth noting that we did not intend to compare the EC and EO conditions, because our assumption was that the linear correlation between the YAO signal and the global signal of fMRI was the same regardless of the EC or EO condition. We collected data under these two conditions because they are dominant paradigms widely used to study the brain resting state.

4.5. Limitations

Our current analyses have several limitations. First, an unsolved problem of simultaneous EEG-fMRI is the low signal-to-noise ratio, and the existing software was unable to thoroughly remove the artifact from EEG. In our study, the average artifact subtraction and ICA were both employed in the artifact correction. However, we also need to be cautious when extending our results to other studies. Second, because of the parameter settings of the fMRI acquisition (interslice gap was employed for the whole brain cover), there were ten percent of the voxels, in which the strength of the BOLD signal was interpolated with the neighbor voxel, and this may affect the estimation of the fMRI global signal. Third, the frequency band of the fMRI signal associated with the YAO signal was less than 0.01 Hz, which was not a major band of the BOLD signal. A serious drawback of this frequency band was that it contained the noise from heart rate, respiration and other artifacts in the MRI environment. To investigate the influence of artifacts in the MRI environment, we recorded the simultaneous EEG-fMRI signal with a phantom, and the data were processed as described in the methods section. The results suggest that the influence of noise was not significant (see Supplementary Figs. S4 and S5 for more information). Fourth, we only tested the correlation between the YAO signal and the global signal of fMRI in EO and EC conditions, and it was unknown whether the high correlation in γ band was reserved in task conditions. Lastly, the YAO signal did not seem to be special in its relationship with the fMRI global signal. As illustrated in Fig. 4, the γ energy of any single electrode is also strongly associated with the fMRI global signal.

5. Conclusion

In conclusion, our current work has three main contributions: (i) we defined a new signal, i.e., the YAO signal, to represent the global signal of EEG; (ii) fMRI global signal fluctuations were positively correlated with high frequencies of power (γ, 30–45 Hz) of the YAO signal, while they were correlated negatively with the low frequencies of power (2–20 Hz) of the YAO signal. There existed correspondence between the YAO signal and fMRI global signal; (iii) the results demonstrated the electrophysiological signatures of global signal from a more macro perspective. More importantly, as the EEG global signal served as an equivalent to the fMRI global signal, it may provide a potential electrophysiological biomarker in neuropsychiatric and other brain illnesses.

Acknowledgements

The authors thank Prof. Dezhong Yao for helpful comments on an earlier version of this manuscript. Research supported by the National Natural Science Foundation of China (Grant No. 31571111), the Chongqing Research Program of Basic Research and Frontier Technology (cstc2017jcyjAX0110) and the > Fundamental Research Funds for the Central Universities (SWU1609109).

Appendix A. Supplementary data

Supplementary material related to this article can be found, in the online version, at doi:https://doi.org/10.1016/j.jneumeth.2018.09.017.

References

Abe, T., Nonomura, T., Komada, Y., Asaoka, S., Sasai, T., Ueno, A., Inoue, Y., 2011. Detecting deteriorated vigilance using percentage of eyelid closure time during behavioral maintenance of wakefulness tests. Int. J. Psychophysiol. 82, 269–274.

Allen, P.J., Josephs, O., Turner, R., 2000. A method for removing imaging artifact from continuous EEG recorded during functional MRI. NeuroImage 12, 230–239.

Ashburner, J., Friston, K.J., 2005. Unified segmentation. NeuroImage 26, 839–851. https://doi.org/10.1016/j.neuroimage.2005.02.018.

Bertrand, O., Perrin, F., Pernier, J., 1985. A theoretical justification of the average reference in topographic evoked potential studies. Electroencephalogr. Clin. Neurophysiol. Potentials Sect. 62, 462–464. https://doi.org/10.1016/0168-5597(85)90058-9.

Bianciardi, M., Fukunaga, M., Van, G.P., Horovitz, S.G., de Zwart, J.A., Shmueli, K., Duyn, J.H., 2009. Sources of functional magnetic resonance imaging signal fluctuations in the human brain at rest: a 7 T study. Magn. Reson. Imaging 27, 1019–1029.
Brazier, M.A.B., 1966. A study of the electrical fields at the surface of the head. Eukaryot. Cell 6, 114–128.
Brookhuis, K., Waard, D., 1993. The use of psychophysiology to assess driver status. Ergonomics 36, 1099–1110.
Dong, L., Li, F., Liu, Q., Wen, X., Lai, Y., Xu, P., Yao, D., 2017. MATLAB toolboxes for reference electrode standardization technique (REST) of scalp EEG. Front. Neurosci. 11, 601. https://doi.org/10.3389/fnins.2017.00601.
Fox, P.T., Raichle, M.E., 1986. Focal physiological uncoupling of cerebral blood flow and oxidative metabolism during somatosensory stimulation in human subjects. Proc. Natl. Acad. Sci. U. S. A. 83, 1140–1144.
Fox, P.T., Raichle, M.E., Mintun, M.A., Dence, C., 1988. Nonoxidative glucose consumption during focal physiological activity. Science 241, 462–464.
Fox, M.D., Snyder, A.Z., Vincent, J.L., Corbetta, M., Van Essen, D.C., Raichle, M.E., 2005. The human brain is intrinsically organized into dynamic, anticorrelated functional networks. Proc. Natl. Acad. Sci. U. S. A. 102, 9673–9678.
Fox, M.D., Zhang, D., Snyder, A.Z., Raichle, M.E., 2009. The global signal and observed anticorrelated resting state brain networks. J. Neurophysiol. 101, 3270–3283.
Friston, K.J., Fletcher, P., Josephs, O., Holmes, A., Rugg, M.D., Turner, R., 1998. Event-related fMRI: characterizing differential responses. NeuroImage 7, 30–40.
Geselowitz, D.B., 1998. The zero of potential. IEEE Eng. Med. Biol. Mag. 17, 128–132.
Goldman, R.I., Stern, J.M., Jr, E.J., Cohen, M.S., 2002. Simultaneous EEG and fMRI of the alpha rhythm. Neuroreport 13, 2487–2492.
Guo, C.C., Kurth, F., Zhou, J., Mayer, E.A., Eickhoff, S.B., Kramer, J.H., Seeley, W.W., 2012. One-year test-retest reliability of intrinsic connectivity network fMRI in older adults. NeuroImage 61, 1471–1483.
Horovitz, S., Fukunaga, M.Z., de Zwart, J.A., Van-Gelderen, P., Fulton, S., Balkin, T., Duyn, J., 2008. Low frequency BOLD fluctuations during resting wakefulness and light sleep: a simultaneous EEG-fMRI study. Hum. Brain Mapp. 29, 671–682.
Kajikawa, Y., Schroeder Charles, E., 2011. How local is the local field potential? Neuron 72, 847–858. https://doi.org/10.1016/j.neuron.2011.09.029.
Khursheed, F., Tandon, N., Tertel, K., Pieters, T.A., Disano, M.A., Ellmore, T.M., 2011. Frequency-specific electrocorticographic correlates of working memory delay period fMRI activity. NeuroImage 56, 1773–1782.
Lachaux, J.P., Fonlupt, P., Kahane, P., Minotti, L., Hoffmann, D., Bertrand, O., Baciu, M., 2007. Relationship between task-related gamma oscillations and BOLD signal: new insights from combined fMRI and intracranial EEG. Hum. Brain Mapp. 28, 1368–1375.
Lei, X., Liao, K., 2017. Understanding the influences of EEG reference: a large-scale brain network perspective. Front. Neurosci. 11, 205. https://doi.org/10.3389/fnins.2017.00205.
Lenkov, D.N., Volnova, A.B., Pope, A.R.D., Tsytsarev, V., 2013. Advantages and limitations of brain imaging methods in the research of absence epilepsy in humans and animal models. J. Neurosci. Methods 212, 195–202.
Liu, Z., Zwart, J.A.D., Yao, B., Gelderen, P.V., Kuo, L.W., Duyn, J.H., 2012. Finding thalamic BOLD correlates to posterior alpha EEG. NeuroImage 63, 1060–1069.
Liu, Q., Balsters, J.H., Baechinger, M., Groen, O.V.D., Wenderoth, N., Mantini, D., 2015. Estimating a neutral reference for electroencephalographic recordings: the importance of using a high-density montage and a realistic head model. J. Neural Eng. 12, 056012.
Logothetis, N.K., Pauls, J., Augath, M., Trinath, T., Oeltermann, A., 2001. Neurophysiological investigation of the basis of the fMRI signal. Nature 412, 150–157.
Mcsweeney, M., Reuber, M., Levita, L., 2017. Neuroimaging studies in patients with psychogenic non-epileptic seizures: a systematic meta-review. Neuroimage Clin. 16, 210–221.
Middlebrooks, E.H., Ver, H.L., Szaflarski, J.P., 2017. Neuroimaging in epilepsy. Curr. Neurol. Neurosci. Rep. 17 (32).
Mishra, A.M., et al., 2011. Where fMRI and electrophysiology agree to disagree: corticothalamic and striatal activity patterns in the WAG/Rij rat. J. Neurosci. 31, 15053–15064.
Mitzdorf, U., 1985. Current source-density method and application in cat cerebral cortex: investigation of evoked potentials and EEG phenomena. Physiol. Rev. 65, 37–100.
Moosmann, M., et al., 2003. Correlates of alpha rhythm in functional magnetic resonance imaging and near infrared spectroscopy. NeuroImage 20, 145–158. https://doi.org/10.1016/S1053-8119(03)00344-6.
Mulert, C., et al., 2010. Single-trial coupling of the gamma-band response and the corresponding BOLD signal. NeuroImage 49, 2238–2247. https://doi.org/10.1016/j.neuroimage.2009.10.058.
Murphy, K., Fox, M.D., 2016. Towards a consensus regarding global signal regression for resting state functional connectivity MRI. NeuroImage 154, 169–173.
Murphy, K., Birn, R.M., Handwerker, D.A., Jones, T.B., Bandettini, P.A., 2009. The impact of global signal regression on resting state correlations: are anti-correlated networks introduced? NeuroImage 44, 893–905.
Niazy, R.K., Beckmann, C.F., Iannetti, G.D., Brady, J.M., Smith, S.M., 2005. Removal of FMRI environment artifacts from EEG data using optimal basis sets. NeuroImage 28, 720–737.
Nunez, P.L., Srinivasan, R., 2006. Electric Fields of the Brain: The Neurophysics of EEG, 2nd ed. Oxford University Press.
Ogawa, S., Lee, T.M., 1990. Magnetic resonance imaging of blood vessels at high fields: in vivo and in vitro measurements and image simulation. Magn. Reson. Med. 16, 9–18.
Olbrich, S., Mulert, C., Karch, S., Trenner, M., Leicht, G., Pogarell, O., Hegerl, U., 2009. EEG-vigilance and BOLD effect during simultaneous EEG/fMRI measurement. NeuroImage 45, 319–332.
Power, J.D., Plitt, M., Laumann, T.O., Martin, A., 2016. Sources and implications of whole-brain fMRI signals in humans. NeuroImage 146, 609–625.
Saad, Z.S., Gotts, S.J., Murphy, K., Chen, G., Jo, H.J., Martin, A., Cox, R.W., 2012. Trouble at rest: how correlation patterns and group differences become distorted after global signal regression. Brain Connect. 2, 25–32.
Scheeringa, R., et al., 2011. Neuronal dynamics underlying high- and low-frequency EEG oscillations contribute independently to the human BOLD signal. Neuron 69, 572–583.
Schölvinck, M.L., Maier, A., Ye, F.Q., Duyn, J.H., Leopold, D.A., 2010. Neural basis of global resting-state fMRI activity. Proc. Natl. Acad. Sci. U. S. A. 107, 10238–10243.
Tyvaert, L., Levan, P., Grova, C., Dubeau, F., Gotman, J., 2008. Effects of fluctuating physiological rhythms during prolonged EEG-fMRI studies. Clin. Neurophysiol. 119, 2762–2774.
Wong, C.W., Olafsson, V., Tal, O., Liu, T.T., 2012. Anti-correlated networks, global signal regression, and the effects of caffeine in resting-state functional MRI. NeuroImage 63, 356–364. https://doi.org/10.1016/j.neuroimage.2012.06.035.
Wong, C.W., Olafsson, V., Tal, O., Liu, T.T., 2013. The amplitude of the resting-state fMRI global signal is related to EEG vigilance measures. NeuroImage 83, 983–990.
Wong, C.W., Deyoung, P.N., Liu, T.T., 2016. Differences in the resting-state fMRI global signal amplitude between the eyes open and eyes closed states are related to changes in EEG vigilance. NeuroImage 124, 24–31.
Yan, L., Zhuo, Y., Ye, Y., Xie, S.X., An, J., Aguirre, G.K., Wang, J., 2009. Physiological origin of low-frequency drift in blood oxygen level dependent (BOLD) functional magnetic resonance imaging (fMRI). J. Soc. Magn. Reson. Med. 61, 819–827.
Yang, G.J., et al., 2014. Altered global brain signal in schizophrenia. Proc. Natl. Acad. Sci. U. S. A. 111, 7438–7443.
Yang, G.J., et al., 2016. Altered global signal topography in schizophrenia. Cereb. Cortex 27, 5156–5169.
Yao, D., 2001. A method to standardize a reference of scalp EEG recordings to a point at infinity. Physiol. Meas. 22, 693–711.
Yao, D., 2017. Is the surface potential integral of a dipole in a volume conductor always zero? A cloud over the average reference of EEG and ERP. Brain Topogr. 30, 161–171. https://doi.org/10.1007/s10548-016-0543-x.
Yeo, T.B., Tandi, J., Chee, M.W., 2015. Functional connectivity during rested wakefulness predicts vulnerability to sleep deprivation. NeuroImage 111, 147–158.
Zarahn, E., Aguirre, G.K., D'Esposito, M., 1997. Empirical analyses of BOLD fMRI statistics. NeuroImage 5, 179–197.